The Impact of Lossless Image Compression to Radiographs

Thomas M. Lehmann[a1], Jürgen Abel[b], and Claudia Weiß[c]

[a] Department of Medical Informatics,
Aachen University of Technology (RWTH), 52057 Aachen, Germany
[b] Ingenieurbüro Dr. Abel GmbH, Lechstr. 1, 41469 Neuss, Germany
[c] Institute of Medical Statistics,
Aachen University of Technology (RWTH), 52057 Aachen, Germany

ABSTRACT

The increasing number of digital imaging modalities results in data volumes of several Tera Bytes per year that must be transferred and archived in a common-sized hospital. Hence, data compression is an important issue for picture archiving and communication systems (PACS). The effect of lossy image compression is frequently analyzed with respect to images from a certain modality supporting a certain diagnosis. However, novel compression schemes have been developed recently allowing efficient but lossless compression.

In this study, we compare the lossless compression schemes embedded in the tagged image file format (TIFF), graphics interchange format (GIF), and Joint Photographic Experts Group (JPEG 2000 II) with the Borrows-Wheeler compression algorithm (BWCA) with respect to image content and origin. Repeated measures ANOVA was based on 1.200 images in total.

Statistically significant effects ($p < 0,0001$) of compression scheme, image content, and image origin were found. Best mean compression factor of 3.5 (2.272 bpp) is obtained applying BTW to secondarily digitized radiographs of the head, while the lowest factor of 1,05 (7.587 bpp) resulted from the TIFF packbits algorithm applied to pelvis images captured digitally. Over all, the BWCA is slightly but significantly more effective than JPEG 2000. Both compression schemes reduce the required bits per pixel (bpp) below 3. Also, secondarily digitized images are more compressible than the directly digital ones. Interestingly, JPEG outperforms BWCA for directly digital images regardless of image content, while BWCA performs better than JPEG on secondarily digitized radiographs. In conclusion, efficient lossless image compression schemes are available for PACS.

Keywords: Lossless Image Compression, Medical Images, Image Databases, Picture Archiving and Communication Systems (PACS), Electronic Healthcare Records (EHR).

1. INTRODUCTION

Improved resolution and novel image modalities rapidly increase the amount of digital image data that needs to be managed in modern healthcare. For instance, university hospitals currently produce more than 2 TB image data per year [1], disregarding optical modalities such as photography, microscopy, endoscopy, and video. Furthermore, this figure is expected to be doubled within the next few years. On the other hand, improved connectivity within the departments of a hospital, interconnectivity to other healthcare providers and applications in telemedicine require fast and efficient transfer of image data in high quality. For example, electronic healthcare records (EHR) are being established that will allow transfer and access to patient's files and images over the Internet.

A lot of work has been published in the field of medical image compression. In general, there are two types of compression schemes:

---

[1] Corresponding author: Priv.-Doz. Dr. Thomas M. Lehmann, Assoc. Prof., Department of Medical Informatics, Aachen University of Technology (RWTH), Pauwelsstr. 30, D - 52057 Aachen, Germany, email: lehmann@computer.org; web: http://irma-project.org/lehmann, phone: +49 241 80-88793.

(i)   lossless compression reduces the file size of an image but results in exactly the same data after decoding,

(ii)   lossy compression modifies the image such that the original pixel values cannot be reconstructed anymore, although the decoded image might look very similar or even identical when compared to it's original.

For a couple of decades, lossless compression of medical images was said to allow a reduction of file size up to the factor 2 or 3 [2], which equals a compression rate CR 2:1 or 3:1, respectively. Since lossy compression allows a significantly larger decrease of the data volume, most papers consider lossy compression techniques. Discrete cosine transform (DCT), e.g., [3,4], and wavelet transform-based algorithms, e.g., [5,6], have been developed and applied for two-dimensional (2D) and three-dimensional (3D) image data, e.g., [7,8]. Beside these rather methodological or technical papers, clinical investigations aim at determining the loss of image quality regarding a certain imaging modality and clinical indication, e.g., [9,10,11]. More precisely, tolerable compression rates of 6:1, 7:1, and 20:1 were found for coronary angiograms [9], digital subtraction radiography in dental radiology [10], and dynamic [18F] 2-flouro-deoxy-glucose brain positron emission tomography data [11], respectively.

Lossless image compression was revisited recently, since computational power of standard computer hardware increased significantly. This allows for computational more expensive compression schemes. In 1996, Kang and Park proposed a multi-level decomposition scheme for lossless compression of medical images [12], and in 1998, a comprehensive comparison of lossless compression methods for medical images was provided by Kivijärvi *et al.* [13].

However, novel lossless coding schemes such as the Borrows-Wheeler compression algorithm (BWCA) or the wavelet-based compression the JPEG[2] 2000 file format were not included in this study. Also, in most of the previous investigations, the number of images analyzed is to small. This also holds for the study in [13], were, for instance only 4 chest radiographs have been included although in total, 3147 images were analyzed. Since it has been shown that the individual content of images is crucial for performance evaluations, e.g., see [14] comparing image interpolation techniques, a large number of images must be analyzed and statistically evaluated. Also, modality, body region, or viewing position might have significant impact to the results obtained. Furthermore, a comparison of lossless compression schemes should regard whether the image data is acquired directly digital or it has been secondarily digitized from film, since the latter might induce artefact correlating to the scanner rather than the images.

In this study, we address these points by using a large but defined dataset of images from different origins, by including recently standardized file formats supporting novel lossless compression schemes, and by providing a reliable statistical analysis. For a more practical point of view, proprietary algorithms are disregarded since not being available in clinical routine. Instead of, the lossless compression schemes embedded in standardized file formats [15] are analyzed and compared to BWCA.

2.   MATERIAL AND METHODS

This section describes the reference database and image categories, the compression schemes, and the statistical analyses performed in this study.

2.1. Image Content and Origin

It is obvious that images obtained from different modalities such as computed tomography, ultrasound, or plain radiography have different entropy and result in different compression rates. However, the body region examined as well as the source of images, which can be either directly digital or secondarily digitized, might also effect the compression rate. Therefore, we selected all radiographs from the IRMA database [16], where at least $n = 120$ images were available in both directly digital and secondarily digitized format showing the same biomedical system in the same body region in the same projection. All images were reduced to 8 bit per pixel (bpp). If more than 120 mages were available, the selection was made arbitrarily. This results in five groups of 240 radiographs (Fig. 1):

1.   11x1-120-200-700, head

2.   11x1-110-414-700, hand

3.   11x3-111-500-000, chest, frontal

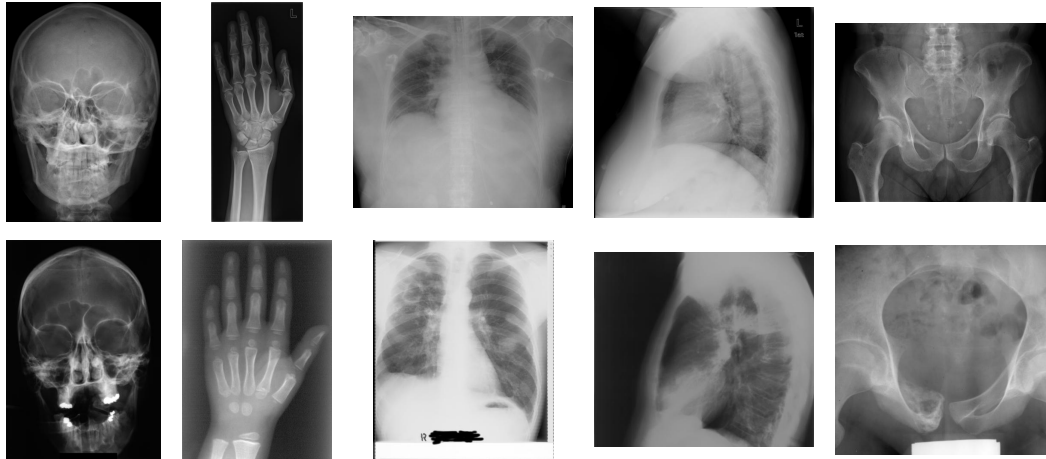[2] JPEG: Joint Photographic Experts Group

Figure 1: Examples of the radiographs in use. Upper row: directly digital, lower row: secondarily captured. From left to right: head; hand; chest, frontal; chest, lateral; pelvis.

> 4.   11x3-211-500-000, chest, lateral
>
> 5.   11x1-120-800-700, pelvis

where MMMM-DDD-AAA-BBB denotes the unique IRMA-code for imaging modality, direction, anatomy, and biosystem, respectively [17]. In the M-part of the code, $x = 1$ and $x = 2$ denotes directly digital and secondarily digitized images, respectively.

2.2. Lossless Data Compression

The image file formats presented in this paper use different data compression schemes. However, all compression schemes are lossless (Tab. 1). Some schemes provide a high throughput but offer only modest compression rates, other schemes reach strong compression rates but execute slowly. In the following, we briefly introduce the different modules of lossless image coding, which are differently combined to effective compression schemes.

Run Length Encoding. Many images contain large amounts of runs for areas with equal color values, e.g. a black background, and store image areas as a sequence of rows. These rows can be efficiently compressed using the run length encoding (RLE) scheme, which is a very simple and fast compression scheme [18]. It replaces runs of repeated symbols by the symbol of the run and the length of the run. However, if the sequence length is only 1, the RLE scheme increases the required storage space for this pixel. Therefore, a special character (e.g., "!") is required to mark whether the following number represents a frequency of repetition or the gray value of the neighbored pixel. In order to guarantee that the compressed image does not increase in data volume, only runs of four or more symbols are converted. For instance, the sequence

         `"ABCAAABCCCCAAAAAAAAAAAAAAAAAAAABBBBC"`   (37 characters)

converts into

         `"ABCAAABC!1A!20B!0C"`   (17 characters)

Here, the special character also defines that the gray value is repeated four times. If a special character is not available in the alphabet, one can – accepting an increase of storage space – use the four-sequence of thy symbol itself. Then, the example above reads to the decoder

         `"ABCAAABCCCC5AAAA20BBBB4C"`   (23 characters)

In these examples, the compression rate is 2.18 and 1.61, respectively.

file format	acronym	compression mode	compression scheme
Windows Bitmap	BMP	---	---
Tagged Image File Format	TIFF	Pack Bits (PB)	RLE
		LZW	LZW
		ZIP	LZW
Graphics Interchange Format	GIF		LZW
Joint Photographic Experts Group (2000)	JPEG-2k		Wavelet
Burrows-Wheeler Compression Algorithm	BWCA		BWCA

Table 1: File formats included in this study and the compression schemes that are embedded.

Dictionary-based Schemes. Dictionary-based schemes like the one of Lempel, Ziv and Welch (LZW) [19], are very popular for image compression. These schemes replace repeating patterns inside the input data by a reference into a dictionary, where the pattern is located. The first time a pattern occurs, the pattern is written into the dictionary and stored. Therefore, the dictionary is build implicitly and does not need to be included in the stored image file.

In contrast to the RLE scheme, LZW schemes compress not only areas with equal gray or color values but also more complex patterns. As a result, LZW schemes achieve stronger compression rates but have a lower speed than RLE schemes.

Wavelet Compression. Wavelet compression schemes as used for the JPEG2000 format are based on the wavelet transform [18]. The wavelet transform splits the image into two different parts. One part contains the low frequency signals of the image and the other the high frequency. These parts are called the scaling and the wavelet function, respectively, while the process of splitting is referred to as a decomposition of the image. The low frequency part can be split recursively by other decompositions. For areas, which contain the same or similar colors, the high frequency part contains many zeroes. These zeroes are independent from the color and can be compressed effectively by a following entropy coding scheme. The entropy coding scheme assigns to each symbol a pattern, which length corresponds to the entropy of that symbol, i.e. to the negative logarithm of the probability of that symbol.

Burrows-Wheeler Compression. The Burrows-Wheeler compression algorithm (BWCA) achieves strong compression rates and a high throughput. The BWCA is a block-oriented scheme that divides the input data into several blocks of a fixed size. In general, the block size ranges from 1 MB to 10 MB. All blocks are processed separately. The BWCA consists of several stages, which are performed sequentially. Each stage transforms the symbols of an input buffer into symbols of an output buffer, which is used as the input buffer for the next stage [20]. The implementation used in this paper consists of four stages (Fig. 2). For decompression, the four stages are executed in reverse order using the inverse schemes each time:

1. the so called Burrows-Wheeler transform (BWT) performs a permutation of the input symbols [21]. In particular, the symbols are reordered according to their following context. Therefore, the output of the BWT stage contains many runs of repeated symbols.

2. a modified RLE scheme, where all runs of size 2 or more are cut into 2 symbols and the length information is passed to a separate run length data stream and compressed separately by an arithmetic coder inside the fourth stage. Consequently, the context of the main output stream is not disturbed by the length information.

3. a so called global structure transform (GST) that transforms the local structure of the RLE main output stream into an index stream with a global structure. Some GST stages use a distance measurement between the occurrence of same symbols like inversion frequencies from Arnavut and Magliveras [22] or distance coding, but most GST stages use a more or less simple frequency ranking scheme similar to the list update problem [23]. The most common approach is the move-to-front stage, which was used in the original scheme by Burrows and Wheeler [21], and which is very fast. Better compression rates are achieved by the more complex weighted frequency count (WFC) stage from Deorowicz [24] and the incremental frequency count (IFC) stage by Abel [25]. In the presented implementation, the IFC stage is used. The compression rates of the IFC stage are in the range of the results of the WFC stage, while the speed is similar to the MTF stage.
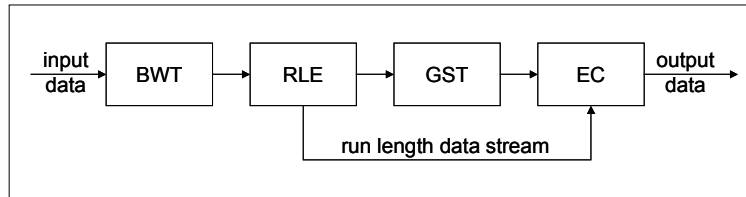
Figure 2: The Burrows-Wheeler Compression Algorithm

4.   an entropy coding (EC) scheme that finally compresses the output of the GST stage into a bit stream. While some EC stages use Huffman coding like BZIP2 [26] or variable length codes [27], we use arithmetic coding [24, 25], which is offering the best compression rates.

2.3. Compression Schemes

For this study, the lossless compression schemes embedded in the most prominent image formats were selected. From the tagged image file format (TIFF), packbits (1. TIF-PB), Lempel-Ziv-Welch (2. TIF-LZW), and ZIP (3. TIF-ZIP) were included. Also, lossless compression of the graphics interchange format (GIF), which is also based on the LZW-algorithm (4. GIF-LZW), and the joint photographic experts group format (JPEG 2000 II), that is based on a wavelet decomposition (5. JPEG-2k), were included in the study. Recently, an efficient block sorting algorithm (6. BWCA) has been proposed for lossless data compression [22] that is based on the Borrows-Wheeler transform [21].

2.4. Statistical Analysis

For all ten groups, means and standard deviations were calculated. Repeated measures analysis of variance (RM-ANOVA) was performed taking into account image origin and content as grouping factors and compression scheme as repeated factor. Statistical analysis was computed using the SAS system (statistical analysis system: SAS 9.1.3, service pack 2, SAS Institute Inc., Cary, NC, USA.). The level of significance was chosen to be alpha = 0.05; adjustment for multiple testing was performed according to Bonferroni. Boxplots are given to show the differences between the image compression algorithms and between the body regions, displaying the mean (plus sign), median, quartiles, and minimum and maximum observations for a group.

3.   RESULTS

Table 2 summarizes the observed compression factors. The effects of compression scheme, image content and image origin were statistically significant overall as well as in post hoc pairwise comparisons of the different compression schemes. Best mean compression factor of 3.5 (2.272 bpp) was obtained applying BWCA to secondarily digitized radiographs of the head, while worst factor of 1,05 (7.587 bpp) resulted from the TIFF packbits algorithm applied to pelvis images captured digitally. Both, BWCA and JPEG-2k require less than 3 bpp, which equals a compression factor of 2.7. For directly digital radiographs, JPEP-2k is significantly better than BWCA regardless of the body region examined, while for secondarily digitized films the results are vice versa.

Figures 3a and 3b show boxplots comparing the six compression algorithms for all body regions taken together, for directly digital and secondarily digitized films respectively. Here it can easily be seen that JPEG-2k and BWCA result in lower size than the other algorithms. Furthermore, highest variability found for TIFF-PB is visualized for both, directly digital and secondarily digitized radiographs. Figures 3c and 3d show the comparison of the different body regions for the example of BWCA. Differences between the body regions, showing highest variability for the hand radiographs, are lower than the differences between the compression algorithms.

4.   DISCUSSION

A comparison of lossless compression methods for medical images was published in 1998 [13]. However, only 4 pediatric chest radiographs were analyzed. In this study, lossless compression of medical images is investigated based

algorithm	image content	directly digital			secondarily digitized			total		
		n	mean	std	n	mean	std	n	mean	std
TIFF-PB	head	120	6.019	0.533	120	7.062	0.240	240	6.540	0.666
	hand	120	7.479	0.881	120	6.944	0.985	240	7.212	0.970
	chest, frontal	120	6.373	0.799	120	4.780	0.739	240	5.577	1.107
	chest, lateral	120	5.594	0.609	120	5.213	0.868	240	5.403	0.772
	pelvis	120	7.587	0.319	120	4.971	1.012	240	6.279	1.509
	total	600	6.610	1.030	600	5.794	1.289	1200	6.202	1.236
TIFF-LZW	head	120	5.189	0.539	120	4.351	0.450	240	4.770	0.649
	hand	120	5.759	0.906	120	4.694	0.614	240	5.226	0.939
	chest, frontal	120	6.194	0.618	120	4.769	0.600	240	5.481	0.938
	chest, lateral	120	5.593	0.591	120	5.123	0.677	240	5.358	0.677
	pelvis	120	6.955	0.496	120	4.978	1.074	240	5.967	1.295
	total	600	5.938	0.882	600	4.783	0.759	1200	5.360	1.005
GIF-LZW	head	120	5.092	0.550	120	4.223	0.470	240	4.658	0.671
	hand	120	5.671	0.906	120	4.599	0.640	240	5.135	0.949
	chest, frontal	120	6.339	0.537	120	4.698	0.532	240	5.519	0.980
	chest, lateral	120	5.624	0.433	120	4.996	0.481	240	5.310	0.555
	pelvis	120	6.872	0.495	120	4.764	0.740	240	5.818	1.229
	total	600	5.920	0.866	600	4.656	0.633	1200	5.288	0.987
TIFF-ZIP	head	120	4.785	0.474	120	4.257	0.417	240	4.521	0.518
	hand	120	5.300	0.762	120	4.534	0.584	240	4.917	0.779
	chest, frontal	120	6.012	0.411	120	4.655	0.499	240	5.334	0.819
	chest, lateral	120	5.449	0.350	120	4.952	0.418	240	5.200	0.458
	pelvis	120	6.246	0.362	120	4.729	0.676	240	5.487	0.933
	total	600	5.558	0.718	600	4.625	0.574	1200	5.092	0.800
JPEG-2k	head	120	2.737	0.368	120	3.170	0.441	240	2.953	0.459
	hand	120	3.222	0.552	120	2.623	0.444	240	2.922	0.583
	chest, frontal	120	3.404	0.414	120	2.398	0.324	240	2.901	0.626
	chest, lateral	120	2.871	0.376	120	2.545	0.254	240	2.708	0.360
	pelvis	120	3.996	0.358	120	2.921	0.399	240	3.458	0.658
	total	600	3.246	0.611	600	2.731	0.469	1200	2.989	0.602
BWCA	head	120	2.900	0.374	120	2.272	0.222	240	2.586	0.440
	hand	120	3.451	0.634	120	2.635	0.409	240	3.043	0.671
	chest, frontal	120	3.511	0.387	120	2.309	0.259	240	2.910	0.686
	chest, lateral	120	2.981	0.368	120	2.488	0.255	240	2.735	0.401
	pelvis	120	4.070	0.357	120	2.470	0.320	240	3.270	0.870
	total	600	3.383	0.606	600	2.435	0.327	1200	2.909	0.680

Table 2: Results. Mean and standard deviation are given in bit per pixel (bpp). They are based on uncompressed images with 8 bpp. Best and worst rate are shaded in green and red, respectively, while the most important figures are shaded yellow. The data that is comparable to [13] is shaded blue.

on a large number of radiographs and profound statistics is applied. It is shown that image content and origin have significant effect on the compression rate. There is a remarkable difference in compressibility between radiographs that have been acquired directly digital and those that have been digitized from x-ray films. Also, we included novel compression schemes such as BWCA and JPEG-2k, which are significantly better than common techniques such as LZW. BWCA outperforms JPEG-2k on the entire set of images as well as on all subsets of secondarily digitized films. In [13], a mean compression ratio of 2.74 was reported for lossless JPEG. Based on a large number of images from different sources and body regions, the mean compression rates turned out to be much lower. In particular, the ratio is 2.35 (3.404 bpp) and 2.28 (3.511 bpp) using JPEK-2k and BWCA, respectively.

5. CONCLUSION

Novel lossless compression schemes such as BWCA or JPEG-2k allow reduction rates of up to 3.5 (2.7 in average) when applied to radiographs. Secondarily digitized x-ray films are more compressible than images from directly digital x-ray modalities.
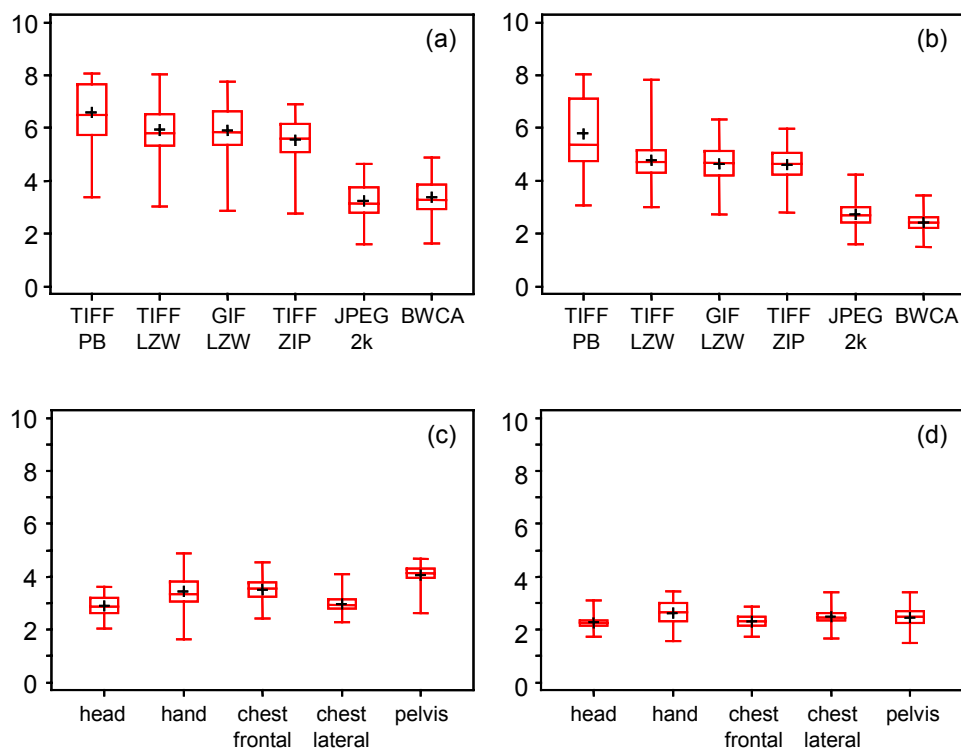
Figure 3: Boxplots for the bit-per-pixel values after compression. (a) all directly digital acquired radiographs; (b) all secondarily digitized radiographs; (c) BWCA compression for directly digital images; (d) BWCA compression for secondarily digitized images.

REFERENCES

1. Müller H, Michoux N, Bandon D, Geissbuhler A: A review of content-based image retrieval systems in medical applications – Clinical benefits and future directions. International Journal of Medical Informatics 2004; 73: 1-23
2. Bruckmann A, Uhl A: Selective medical image compression techniques for telemedical and archiving applications. Computers in Biology and Medicine 2000; 30: 153-69
3. Wu YG, Tai SC: Medical image compression by discrete cosine transform spectral similarity strategy. IEEE Transactions on Information Technology in Biomedicine 2001; 5(3): 236-43
4. Wu YG: Medical Image Compression by Sampling DCT Coefficients. IEEE Transactions on Information Technology in Biomedicine 2002; 6(1): 86-94
5. Schomer DF, Elkes AA, Hazle JD, Huffman JC, Thompson SK, Chui CK, Murphy WA: Introduction to wavelet-based compression of medical images. RadioGraphics 1998; 18: 469-81
6. Phelyn NC, Ennis JT: Medical image compression based on a morphological representation of wavelet coefficients. Medical Physics 1999; 26(8): 1607-11
7. Tai SC, Wu YG, Lin CW: An adaptive 3-D discrete cosine transform coder for medical image compression. IEEE Transactions on Information Technology in Biomedicine 2000; 4(3): 259-63

8. Schelkens P, Munteanu A, Barbarien J, Galca M, Giro-Nieto X, Cornelis J: Wavelet coding of volumetric medical datasets. IEEE Transactions on Medical Imaging 2003; 22(3): 441-58
9. Brennecke R, Bürgel U, Simon R, Rippin G, Fritsch HP, Becker T, Nissen SE: American College of Cardiology / European Society of Cardiology international study of angiographic data compression phase III. Journal of the American College of Cardiology 2000; 35: 1388-97 / European Heart Journal 2000; 21: 687-96
10. Fidler A, Likar B, Pernus F, Skaleric U: Comparative evaluation of JPEG and JPEG2000 compression techniques in quantitative digital subtraction radiography. Dentomaxillofacial Radiology 2002; 31: 379-84
11. Feng D, Cai W, Fulton R: Dynamic image compression in the spatial and temporal domains – Clinical issues and assessment. IEEE Transactions on Information Technology in Biomedicine 2002; 6(4): 262-8
12. Kang KS, Park HW: Lossless medical image comparison by multilevel decomposition. Journal of Digital Imaging 1996; 9(1): 11-20
13. Kivijarvi J, Ojala T, Kaukoranta T, Kuba A, Nyul L, Nevalainen O: A comparison of lossless compression methods for medical images. Computerized Medical Imaging and Graphics 1998; 22(4): 323-39
14. Lehmann TM, Gönner C, Spitzer K: Survey: Interpolation methods in medical image processing. IEEE Transactions on Medical Imaging 1999; 18(11): 1049-75
15. Wiggins RH, Davidson HC, Harnsberger HR, Lauman JR, Goede PA: Image file formats – Past, present, and future. RadioGraphics 2001; 21: 789-98
16. Lehmann TM, Güld MO, Thies C, Fischer B, Spitzer K, Keysers D, Ney H, Kohnen M, Schubert H, Wein BB: Content-based image retrieval in medical applications. Methods of Information in Medicine 2004; 43(4): 354-61
17. Lehmann TM, Schubert H, Keysers D, Kohnen M, Wein BB: The IRMA code for unique classification of medical images. Procs SPIE 2003; 5033: 440-51
18. Sayood K: Introduction to Data Compression, Academic Press, 2nd edition, 2000.
19. Ziv J, Lempel A: A universal algorithm for sequential data compression. IEEE Transactions on Information Theory 1977; 23; 337-42
20. Sayood K (ed): Lossless Compression Handbook. Academic Press, 2003.
21. Burrows M, Wheeler DJ: A Block-Sorting Lossless Data Compression Algorithm. Technical Report, Digital Equipment Corporation, Palo Alto, California, 1994 (http://citeseer.ist.psu.edu/76182.html).
22. Arnavut Z, Magliveras SS: Block sorting and compression. Proceedings of the IEEE Data Compression Conference 1997, Snowbird, Utah, 1997; 181–190.
23. Bentley J, Sleator D, Tarjan R, Wei V. A locally adaptive data compression scheme. Communications of the ACM 1986; 29: 320-30
24. Deorowicz S: Second step algorithms in the Burrows-Wheeler compression algorithm. Software – Practice and Experience 2002; 32(2): 99-111
25. Abel J. A fast and efficient post BWT-stage for the Burrows-Wheeler Compression Algorithm. Proceedings of the IEEE Data Compression Conference 2005, Snowbird, Utah, 2005; 449
26. Seward J: On the performance of BWT sorting algorithms. Proceedings of the IEEE Data Compression Conference 2000, Snowbird, Utah, 2000; 173-82
27. Fenwick P: Burrows Wheeler compression with variable length integer codes. Software – Practice and Experience, 2002; 32(13): 1307-16